

CHARACTERIZATION OF THE ELASTIC CONSTANTS OF UNIDIRECTIONAL LAMINATES USING OBLIQUE-INCIDENCE PULSED DATA

Ajit K. Mal and Shyh-Shiuh Lih
Mechanical, Aerospace and Nuclear Engineering Department
University of California Los Angeles, California

Yoseph Bar-Cohen
Jet Propulsion Laboratory, California Institute of Technology
Pasadena, California

INTRODUCTION

Composites are increasingly applied for fabrication of fracture-critical structures and their subcomponents with graphite/epoxy as the most widely used material in aircraft structures. These materials provide an effective combination of toughness, specific strength, modulus and damage tolerance. However, composites are very sensitive to their manufacturing processes, service conditions and the natural environment, either one or all of which may introduce defects resulting in a serious degradation of the material. Further, as these materials age, their properties are degraded and it becomes increasingly critical to nondestructively evaluate them for repair or reject.

Ultrasonics offer the most capable inspection technology" and several recently developed techniques appear to have the potential of significantly improving the state-of-the-art in NDE technology. Particularly capable is the leaky Lamb wave (LLW) technique, in which a specimen is immersed in water and is tested by two broadband ultrasonic transducers in a pitch-catch arrangement. In this method, a variety of waves are generated within the specimen and each of these waves carries specific information on the characteristics of the material. Careful analysis of the recorded waveforms can, in principle, unravel this information [1-3].

In this paper, we apply the LLW technique to determine the stiffness constants of unidirectional graphite/epoxy materials. A systematic procedure was proposed by Karim, Mal and Bar-Cohen [4] through an inversion of the LLW dispersion data was determined as an effective method to characterize the elastic constants of graphite/epoxy composites. The authors' careful parameter study showed that this method can only be used to accurately determine the matrix dominated stiffness constants c_{22} , c_{33} and c_{55} . Due to the fact that the Lamb wave velocity is insensitive to c_{11} and c_{12} in the range in which the dispersion data are reliable, these fiber dominated constants can not be determined accurately by this procedure.

In this paper, we describe a new technique which can be used to determine all five stiffness constants by analyzing the times-of-flight of the recorded reflected acoustic waves in a pulsed LLW experiment. A generalized ray theory described in Mal *et al.* [5] is used to identify the modality and ray path of each arrival; the time of flight of each ray is then related to the elastic constants of the composite. The accuracy of the inversion procedure is discussed.

THE ULTRASONIC EXPERIMENT

The general principle of the experiment is the use of an ultrasonic pitch-catch arrangement with an access to the test material from a single side. An ultrasonic broadband wave insonifies the specimen, immersed in water, at an oblique angle and the reflected signals are received by a second transducer. A description of the set-up was shown earlier in the literature, for example see Fig. 1. A number of flat, broadband transducers with center frequencies in the range of 0.5 - 10 MHz are used and the signals, transmitted either in tone-burst or short pulse form, are used to study the material characteristics.

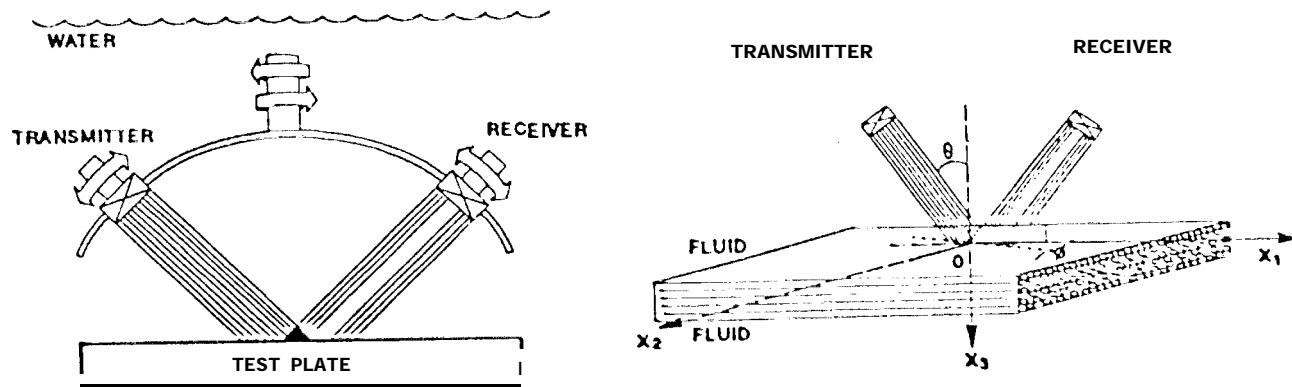


Fig. 1: The experimental set-up.

The test signals are generated by a function generator HP8116A to establish a steady-state condition. At specific angles of incidence the reflected signal is recorded as a function of frequency, amplified, averaged and digitized with the aid of an SRS gated integrator. The amplitude spectrum of the reflected signal is obtained by changing the frequency of the tone-burst signal over the individual transducers' effective spectral range. For angle of incident, θ , that are greater than certain critical value, multi-modal dispersive guided waves are induced in the specimen at a finite number of specific frequencies of excitation. The guided waves propagate in a direction parallel to the surfaces of the specimen and leak energy into the surrounding fluid. The leaky waves interfere with the specularly reflected wave to form minima or "nulls" in the amplitude spectra of the reflected signal at the modal frequencies of the guided waves. The phase velocity, V , of the guided waves is related to the angle of incidence, θ , through Snell's law:

$$V = \alpha_0 / \sin \theta$$

where α_0 is the acoustic wave speed in the fluid. Thus, for a given angle of incidence, the minima or nulls in the reflection amplitude spectrum are associated with the excitation of leaky guided waves in the specimen. Dispersion curves for the specimen are determined from the minima frequency as a function of the phase velocity. The material constants and the thickness of the specimen are related to the dispersion curves and can be determined by fitting the experimental curves with those obtained from theory.

In the second method, pulsed signals are transmitted in either a pulse-echo or pitch-catch arrangement [3]. The reflected signals in the time-domain are recorded and if there is clear separation between the individual pulses, their measured times-of-flight are used to determine the material constants through analysis.

CHARACTERIZATION OF MATERIAL CONSTANTS FROM LLW EXPERIMENT

The basic idea behind the technique [4] is to obtain the experimental LLW dispersion curves for the test specimen for which the theoretical dispersion curves can be determined using the expected five stiffness constants of the specimen. Then, the specimen stiffness constants are determined consistently by "best fit" between the theoretical and measured curves. As an example, a unidirectional 1 mm thickness graphite/epoxy laminate was tested both experimentally and theoretically for waves propagating at 0° , 45° and 90° to the fibers. The material constants were determined from inversion and they are as follows:

$$c_{11} = 160.73, c_{12} = 6.44, c_{22} = 13.92, c_{23} = 6.92, c_{33} = 7.07 \quad (\text{units in GPa})$$

Overall, the data obtained for unidirectional, cross-ply and quasi-isotropic graphite/epoxy laminates were

documented in the literature and have shown a very good fit between the measured and calculated dispersion curves [4-5]. However, the relation between the calculated wave speed and the unknown stiffness constants is highly nonlinear and the solution to the inversion problem is nonunique. In addition, each stiffness constant has a different influence on the dispersion curves, and this can affect the accuracy of its estimated value. Data errors also play an important role in the inversion algorithm. These issues have not been carefully studied.

A detailed and systematic parameter study was carried out to determine the influence of the five stiffness constants on the dispersion curves. The authors examined both the symmetric and antisymmetric Lamb wave modes for wave propagation at 0°, 45° and 90° to the fibers. Changes in c_{22} , c_{23} , c_{55} have shown a strong influence on all modes of the dispersion curves, while c_{11} only affected the first symmetric mode at the high velocity range. Tests at the high velocity range require small incidence angles ($\leq 10^\circ$) which are difficult and time-consuming to set experimentally, and the errors in locating the minima in the dispersion curves are large. Further, the constant c_{12} does not seem to have significant influence on any of the modes. Thus, practically only three constants c_{22} , c_{23} , and c_{55} can be determined accurately from the dispersion curves. The authors examined the feasibility of using time-domain data as an alternative technique to obtain accurate estimates of all five constants and, at the same time, is simpler to implement both in the laboratory and in field environments.

CHARACTERIZATION OF THE MATERIAL CONSTANTS FROM TIME-DOMAIN DATA

Ray theory. Consider a unidirectional composite plate with thickness H and density ρ immersed in a fluid as shown in Fig. 1. Assume that the material is homogeneous and transversely isotropic with symmetry axis along x_1 and characterized by five stiffness constants, c_{11} , c_{12} , c_{22} , c_{23} , and c_{55} . The Cauchy's equation of motion for the material is

$$\sigma_{ij,j} - \rho \ddot{u}_i = 0 \quad (1)$$

where u_i is the displacement vector and σ_{ij} is the stress tensor. Assume plane wave solutions of (1) in the form

$$u_i = U_i e^{i(k_1 x_1 + k_2 x_2 + k_3 x_3) - i\omega t} \quad (2)$$

where k_1 , k_2 and k_3 represent the wavenumbers along the x_1 , x_2 and x_3 directions, respectively, and ω is the circular frequency. From (1), (2) and the constitutive relations for the material we obtain the following eigenvalue problem for calculation of the wave speed in a given direction:

$$\begin{bmatrix} a_2 \xi_1^2 + a_3 (\xi_2^2 + \zeta^2) - 1 & a_3 \xi_1 \xi_2 & a_3 \xi_1 \zeta \\ a_3 \xi_1 \xi_2 & a_3 \xi_1^2 + a_1 \xi_2^2 + a_4^2 \zeta^2 - 1 & (a_1 - a_4) \xi_2 \zeta \\ a_3 \xi_1 \zeta & (a_1 - a_4) \xi_2 \zeta & a_3 \xi_1^2 + a_4 \xi_2^2 + a_1 \zeta^2 - 1 \end{bmatrix} \begin{Bmatrix} U_1 \\ U_2 \\ U_3 \end{Bmatrix} = \begin{Bmatrix} 0 \\ 0 \\ 0 \end{Bmatrix} \quad (3)$$

where

$$\begin{aligned} a_1 &= c_{22}/\rho, & a_2 &= c_{11}/\rho, & a_3 &= (c_{12} + c_{55})/\rho, & a_4 &= (c_{22} - c_{23})/2\rho, & a_5 &= c_{55}/\rho \\ \xi_1 &= k_1/\omega, & \xi_2 &= k_2/\omega, & \zeta &= k_3/\omega \end{aligned} \quad (4)$$

In the ultrasonic experiment, ξ_1 and ξ_2 are related to the incident angle θ and fiber orientation ϕ in the form

$$\xi_1 = \frac{\sin \theta \cos \phi}{\alpha_0}, \quad \xi_2 = \frac{\sin \theta \sin \phi}{\alpha_0} \quad (5)$$

where α_0 is the acoustic wave speed in water (≈ 1.485 mm/ μ s). Then, ζ is given by the condition of nontrivial solutions of (3). It can be shown that there are three values of ζ , giving rise to three rays in a given direction:

$$\zeta_k = \sqrt{b_k - \xi_2^2} \quad (k = 1, 2, 3) \quad (6)$$

where

$$b_1 = -(\beta/2\alpha) - \sqrt{(\beta/2\alpha)^2 - \gamma/2\alpha}, \quad b_2 = -(\beta/2\alpha) + \sqrt{(\beta/2\alpha)^2 - \gamma/2\alpha}, \quad b_3 = \frac{1 - a_3\xi_1^2}{a_4} \quad (7)$$

$$\alpha = a_1 a_5, \quad \beta = (a_1 a_2 + a_5^2 - a_3^2)\xi_1^2 - (a_1 + a_5), \quad \gamma = (a_2 \xi_1^2 - 1)(a_3 \xi_1^2 - 1)$$

The ray diagram for a plane wave transmitted into a unidirectional composite plate is shown in Fig. 2a. Here R^0 indicates the first reflected wave from the top surface of the plate, the rays labeled 1, 2, 3 are associated with the three transmitted waves inside the plate in a decreasing order of their speeds, the rays labeled 11, 12, ..., and 33 are associated with the waves reflected from the bottom of the plate, and T_1, T_2, T_3 indicate the waves transmitted into the fluid through the bottom of the plate. From Snell's law, the velocities V_k, V , and the angles θ_k, θ_l in the diagram are related through

$$\frac{\sin \theta_0}{V_k} = \frac{\sin \theta_k}{V} \quad (8)$$

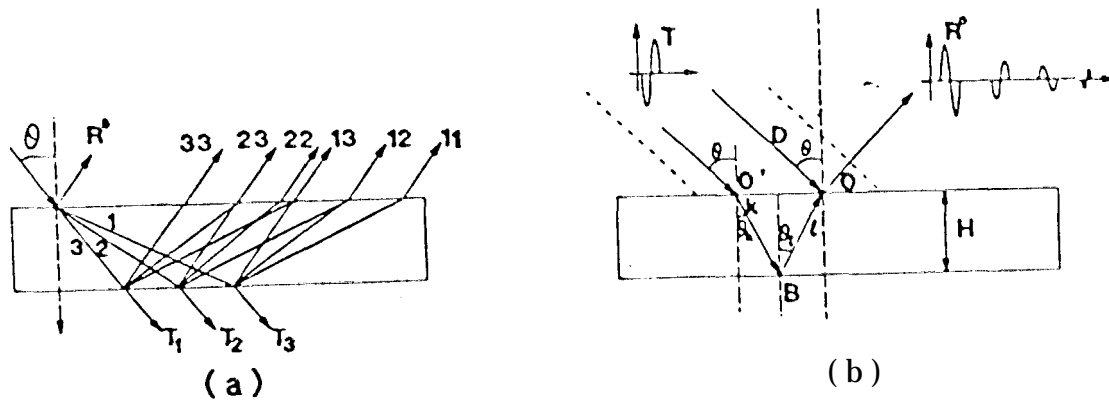


Fig. 2. Ray diagrams of the reflected waves in a unidirectional composite laminate.

Two possible ray paths leading to the same point on the receiver are sketched in Fig. 2b. If we denote the difference in the arrival times between rays along paths DO and O'BO by t_M , then t_M can be expressed as

$$t_M = t_k + t_l - t^D \quad (9)$$

where

$$t_k = \frac{H}{V_k \cos \theta_k}, \quad t_l = \frac{H}{V_l \cos \theta_l}, \quad t^D = \frac{H(\tan \theta_k + \tan \theta_l) \sin \theta_0}{\alpha_0} \quad (10)$$

From (9) and (10), t_M can be expressed as

$$t_M = \frac{H}{V_k \cos \theta_k} - \frac{H}{V_l \cos \theta_l} - \frac{H(\tan \theta_k + \tan \theta_l) \sin \theta_0}{\alpha_0} = \frac{H \cos \theta_k}{V_k} + \frac{H \cos \theta_l}{V_l} = H(\zeta_k + \zeta_l) \quad (11)$$

It should be noted that equation (11) is valid for homogeneous waves only, i.e., when ζ_k, ζ_l are real. In general, there are three possible bulk wave speeds in a composite material, and the recorded time history should contain a reflected pulse from the top surface followed by nine reflected rays from the bottom of the plate and their multiple reflections. However, for a fixed orientation ϕ to the fibers, a certain homogeneous wave will become inhomogeneous or evanescent if the incident angle θ is larger than the critical incident angle θ_c . Analysis of

waves propagating along the fiber ($\phi = 0^\circ$) with different incident angles shows that for the pulse-echo ($\theta = 0^\circ$) case only the longitudinal waves exist so that the reflected pulses are "11", "1111" etc. As the incident angle θ increases, the mode converted reflected pulses become more significant. When $\theta \approx 8^\circ$, all of the pulses can be identified clearly. Whereas for $\theta > \theta_c (\approx 8.4^\circ)$ the pulses with velocity V , disappear, and the most prominent pulse is "22".

Since the wave speed in a composite material is a function of the orientation ϕ , it is possible to have critical values of ϕ for a fixed value of θ . Thus, some of the homogenous waves may become evanescent when the propagation angle ϕ is larger or smaller than a certain critical angle ϕ_c .

THE Experimental Procedure - Based on the above theory, an experimental procedure was formulated to determine the five stiffness constants.

a) Pulse-echo experiment - In this case, $\xi_1 = \xi_2 = 0$, so that from (4)-(7)

$$\zeta_1 = \sqrt{\rho/c_{22}}, \quad \zeta_2 = \sqrt{\rho/c_{55}}, \quad \zeta_3 = \sqrt{2\rho/(c_{22} - c_{23})} \quad (12)$$

and the corresponding eigenvectors for ζ_1, ζ_2 , and ζ_3 are $(0, 0, 1)$, $(0, 1, 0)$ and $(1, 0, 0)$. Since only the longitudinal wave can be transmitted into the fluid from the composite, only the rays associated with ζ_1 exist. Hence the first pulse must be "11", and its arrival time is t_{11} . From (11) and (12),

$$c_{22} = \rho/\zeta_1^2 = 4\rho H^2/t_{11}^2 \quad (13)$$

Thus the pulse-echo experiment provides the constant c_{22} , where $t_{11} = 16.83 \mu\text{s}$. Then, c_{22} is found from (13) to be 13.92 GPa , in agreement with the value used in the theoretical calculation.

b) Oblique insonification with $\phi = 90^\circ$ and incident angle $\theta > 0^\circ$ - In this case,

$$\xi_1 = 0, \quad \xi_2 = \sin \theta / \alpha_0, \quad b_1 = 1/a_1, \quad b_2 = 1/a_3, \quad b_3 = 1/a_4 \quad (14)$$

and

$$\zeta_1^2 = -\xi_2^2 + 1/a_1, \quad \zeta_2^2 = -\xi_2^2 + 1/a_3, \quad \zeta_3^2 = -\xi_2^2 + 1/a_4 \quad (15)$$

It should be noted that the eigenvector associated with ζ_2 is $(1, 0, 0)$, indicating that the particle motion is parallel to the fibers, and this transverse wave can not be transmitted into the fluid. Hence, there is no pulse associated with the COMPLEX MODE ray path, and the arrived pulses should be in the sequence "11", "13", and "33". In this experiment, the direction ϕ is kept fixed and the incident angle is increased from 0° until the pulses "11" and "13" can be identified clearly and t_{11} and t_{13} can be measured. The constants c_{22} and c_{23} can be determined from the formulas,

$$c_{22} = \frac{\rho}{\left(\frac{t_{11}}{2H}\right)^2 + \frac{\sin^2 \theta}{\alpha_0^2}}, \quad c_{23} = c_{22} - \frac{2\rho}{\left(\frac{t_{13}}{H} - \frac{t_{11}}{2H}\right)^2 + \frac{\sin^2 \theta}{\alpha_0^2}} \quad (16)$$

Then c_{22} and c_{23} can be calculated from (16) as 13.92 GPa and 6.92 GPa , respectively

c) Oblique insonification with ϕ less than the critical angle ϕ_c .

After c_{22} and c_{23} have been determined, the constant c_{33} can be found as follows. With fixed incident angle θ , adjust ϕ such that the pulses "22" and "23" can be identified clearly. Then from measured t_{22} , c_{33} can be

determined from the formula,

$$c_{55} = - \frac{\rho \alpha_0^2}{\sin^2 \theta \cos^2 \phi} \left\{ 1 - \frac{(c_{22} - c_{23})}{2\rho} \left[\left(\frac{t_{23}}{H} - \frac{t_{22}}{2H} \right)^2 + \frac{\sin^2 \theta \sin^2 \phi}{\alpha_0^2} \right] \right\} \quad (17)$$

Hence c_{55} can be determined from (17) as 7.08 GPa.

d) Oblique insonification with $\phi = 0$

The remaining two unknowns c_{11} and c_{12} , can be determined from this procedure. The time of flight t_{11} and t_{12} can be identified by changing θ from 0° to an angle less than the first critical angle θ_c . Then ξ_1 and ξ_2 can be calculated from (6) and c_{11} and c_{12} can be determined from the equations,

$$c_{11} = \left[- \frac{\alpha_0^2 c_{22} c_{55}}{\rho (c_{55} \sin^2 \theta - \rho \alpha_0^2) \left(\frac{t_{11}}{2H} \right)^2} \left(\frac{t_{12}}{H} - \frac{t_{11}}{2H} \right)^2 + 1 \right] \frac{\rho \alpha_0^2}{\sin^2 \theta} \quad (18)$$

$$c_{12} = \left\{ (c_{11} c_{22} + c_{55}^2) - \frac{\alpha_0^2}{\sin^2 \theta} \left[\rho (c_{22} + c_{55}) - c_{11} c_{55} \left(\left(\frac{t_{11}}{2H} \right)^2 + \left(\frac{t_{12}}{H} - \frac{t_{11}}{2H} \right)^2 \right) \right] \right\}^{1/2} - c_{55}$$

Then, c_{11} and c_{12} are calculated from (18) to be 161.8 GPa and 6.46 GPa, respectively.

Since experiment d) is difficult to carry out due to the small incident angle θ , an alternate method is proposed to determine the remaining constant c_{11} and c_{12} . Our calculations have shown that the reflected field changes significantly near the critical angle.

The arrival times of these pulses are strongly affected by c_{11} near critical angle. We use this critical angle phenomenon to determine the constants c_{11} and c_{12} . Recall that the equation for the bulk wave speed V associated with the constants c_{11} and c_{12} can be written as

$$[(a_1 - a_5) + (a_5 - V^2)^2 / n_2^2] a_2 - a_3^2 = - [(a_5 - V^2)^2 + (a_5 - V^2)(-a_5 + a_1 n_2^2) + a_5(a_1 - a_5) n_1^2 n_2^2] / n_1^2 n_2^2$$

where $n_1 = \cos \phi$, $n_2 = \sin \phi$. The constants a_1, a_4, a_5 can be derived from the known constants c_{22}, c_{23}, c_{55} , and the remaining unknowns a_2 and a_3^2 can be related to c_{11} and c_{12} through Eq. (4). In the critical cases $\phi = \phi_c$ and $V = \alpha_c / \sin \theta$. Hence if we can determine two critical angles from the experiment then the unknowns a_2 and a_3^2 can be calculated from a system of linear equations. In this case, the two critical angles are $\phi_c = 57.67^\circ$ for $\theta = 15^\circ$, and $\phi_c = 68.10^\circ$ for $\theta = 20^\circ$, so that c_{11} and c_{12} can be calculated as 161.12 and 6.14 GPa., respectively.

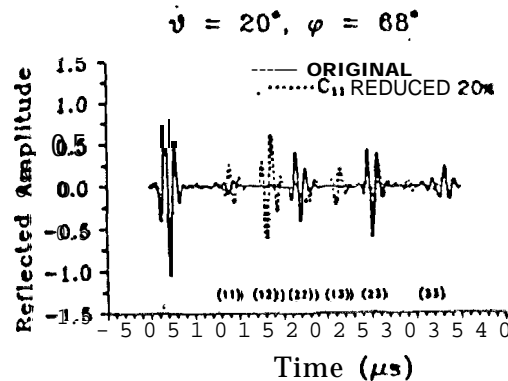


Fig. 3. Influence of the stiffness constant c_{11} on the reflected signal

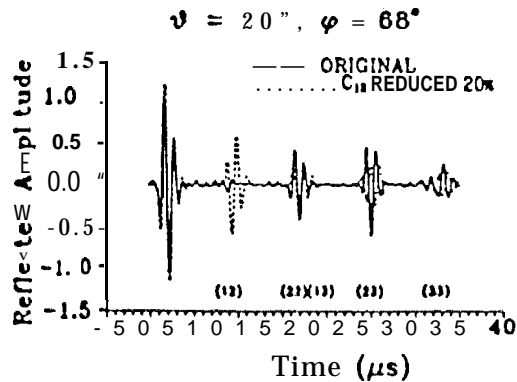


Fig. 4. Influence of the stiffness constant c_{12} on the reflected signal.

Error Analysis - An error analysis is carried out in each step of the experiments to determine the accuracy of the time-domain technique as follows:

a) Pulse-echo experiment

$$\delta c_{22} = -(c_{22}/2t_{11})\delta t_{11} \quad \text{If } \delta = \pm 0.02 \mu\text{s, then } \delta c_{22} = \pm 0.0082 \text{ GPa}$$

b) Oblique insonification with $\phi = 90^\circ$ and incident angle $\theta > 0^\circ$

$$\delta c_{23} = \delta c_{22} + \frac{2(c_{22} - c_{23})}{(\xi_2^2 + \zeta_3^2)^2} (\xi_2 \delta \xi_2 + \zeta_3 \delta \zeta_3)$$

where $\delta \xi_2 = \cos \theta \delta \theta / \alpha_0$, $\delta \zeta_3 = (\delta t_{13} - \delta t_{33} / 2) / H$. If $\delta \theta = \pm 0.1^\circ$ and $\delta t = 0.02 \mu\text{s}$, then $\delta c_{23} = \pm 0.012 \text{ GPa}$.

c) Oblique insonification with ϕ less than the critical angle ϕ_c .

$$\delta c_{55} = \{-2(c_{22} - c_{23})[(\zeta_3^2 + \xi_2^2)\delta \xi_1 / \xi_1 + (\zeta_3 \delta \zeta_3 + \xi_2 \delta \xi_2)] + (\delta c_{22} - \delta c_{55})(\zeta_2^2 + \xi_2^2) / \xi_1^2\}$$

If $\delta \theta = \pm 0.1^\circ$ and $\delta t = 0.02 \mu\text{s}$, then $\delta c_{55} = \pm 0.11 \text{ GPa}$. From the above analysis, it can be seen that the constants determined in steps (a), (b) and (c) are very accurate and small errors in the data have small effects on the constants c_{11} and c_{12} .

a) Oblique insonification with $\phi = 0^\circ$

Since the equations for the determination of the constants c_{11} and c_{12} are very complicated, numerical estimates of the errors analysis were carried out and are presented in Fig. 15. It can be seen that the errors in both cases are smaller than 10% if δt_{11} and δt_{12} are less than $0.1 \mu\text{sec}$. The errors in c_{11} remain very small for δt_{11} and δt_{12} up to $0.5 \mu\text{sec}$. However, the error in c_{12} becomes very large when δt becomes larger. Hence, it is necessary to control the accuracy of the arrival time under $0.1 \mu\text{s}$ to accurately evaluate c_{12} .

e) Critical angle experiment:

As in d) it is difficult to obtain analytical estimates of the errors in an explicit form in this case. So we computed the errors by changing measured ϕ and θ by small amounts near the critical angles. For $\delta \theta = \pm 0.1^\circ$ and $\delta \phi_c = \pm 0.1^\circ$ the error is $c_{11} = 161.12 \pm 2.0 \text{ GPa}$ and $c_{12} = 6.14 \pm 0.8 \text{ GPa}$. We can see that the errors in c_{11} and c_{12} induced by measurement errors are small. Hence, this procedure can be an accurate method for practical application.

CONCLUDING REMARKS

The proposed method appears to be efficient and accurate in characterizing all 5 stiffness constants of a unidirectional fiber-reinforced composite laminate. The error analysis shows that the determined constants are insensitive to small errors in the data. Extension of work will provide a nondestructive procedure that can determine the degree of materials degradation in unidirectional as well as multilayered composite systems.

ACKNOWLEDGMENTS

This research was supported by the Mechanics Division of the Office of Naval Research under Contract N00014-90-1-1857 monitored by Dr. Yapa D. S. Rajapakse. The portion of work carried out by the Jet Propulsion Lab was performed under a contract with the National Aeronautics and Space Administration.

REFERENCES

1. Mal, A.K. and Bar-Cohen, Y., "Nondestructive Characterization of Composite Laminates," *Proceedings of the Mechanics of Composites Review*, Dayton, Ohio, pp. 151-159, 1991.
2. Bar-Cohen, Y., "Ultrasonic NDE of Composite - a Review," *Solid Mechanics Research for Quantitative NDE*, J.D. Achenbach and Y. Rajapakse (Eds.), Martinus Nijhoff Publishers, Boston, pp. 197-201, 1987.
3. Mal, A. K., Gorman, M. R., and Prosser, W. H., "Material Characterization of Composite Laminates Using Low-frequency Plate Wave Dispersion Data," *Review of Progress in Quantitative NDE*, Vol. 11, pp. 1451-1458, 1992.
4. Karim, M. R., Mal, A. K., and Bar-Cohen, Y., "Inversion of Acoustic Wave Data by Simplex Algorithm," *J. Acoust. Soc. Am.*, Vol. 88, pp. 482-491, 1990.
5. Mal, A. K., Yin, C.-C., and Bar-Cohen, Y., "Analysis of Acoustic Pulses Reflected from the Fiber-Reinforced Composite Laminates," *J. Appl. Mech.* Vol. 59, No. 2, pp. 136-144, 1992.